

Brown, A.J., Chen, D., "Probabilistic Method for Predicting Ship Collision Damage", *Ocean Engineering International Journal*, Vol. 6 No. 1, pp. 54-65, 2002.

Probabilistic Method for Predicting Ship Collision Damage

Alan Brown¹ and Donghui Chen²

¹Professor of Aerospace and Ocean Engineering
Department of Aerospace and Ocean Engineering
Virginia Polytechnic Institute and State University
Blacksburg, VA 24061-0203, USA
(540) 231-4950
Fax: (540) 231-9632
brown@aoe.vt.edu

²Student
Department of Aerospace and Ocean Engineering
Virginia Polytechnic Institute and State University

ABSTRACT

This paper describes a method for developing probability density functions (pdfs) describing struck ship damage in ship collisions. Struck and striking ship speed, collision angle, striking ship type and striking ship displacement are treated as independent random variables in this problem. Other striking ship characteristics are treated as dependent variables derived from the independent variables based on relationships developed from worldwide ship data. A simplified collision model (SIMCOL) is used in a Monte Carlo simulation to predict probabilistic damage extents. SIMCOL applies the scenario variables directly in a time-stepping simultaneous solution of internal (structural) deformation and external (ship) dynamics. Results are presented for collisions with four notional tankers designs.

1. INTRODUCTION

The serious consequences of ship collisions necessitate the development of regulations and requirements for the subdivision and structural design of ships to minimize damage, reduce environmental pollution, and improve safety. The Society of Naval Architects and Marine Engineers (SNAME) Ad Hoc Panel #6 was established to study the effect of structural design on the extent of damage in ship collision and grounding. SNAME and the Ship Structure Committee (SSC) sponsor the research under this panel that is presented in this paper.

The International Maritime Organization (IMO) is responsible for regulating the design of oil tankers and other ships to provide for ship safety and environmental protection. Their ongoing transition to probabilistic performance-based standards requires the ability to predict the probabilistic environmental performance and safety of specific ship designs. This is a difficult problem requiring the application of fundamental engineering principles and risk analysis.

IMO first introduced probabilistic standards in damage stability regulations for passenger ships [IMCO 1973] and later for cargo ships [Gilbert and Card 1990]. IMO's first attempt to apply a probabilistic methodology to tankers was in response to the US Oil Pollution Act of 1990 (OPA 90). In OPA 90 the US required that all oil tankers entering US waters must have double hulls. IMO responded to this unilateral action by requiring double hulls or their equivalent. Equivalency is determined based on probabilistic oil outflow calculations specified in [IMO 1995]. All of these regulations use probability density functions (pdfs) to describe the location, extent and penetration of side and bottom damage. These pdfs are derived from limited historical damage statistics [IMO 1989], and applied identically to all ships without consideration of their structural design.

A major shortcoming in IMO's current oil outflow and damage stability calculation methodologies is that they do not consider the effect of structural design or crash-worthiness on damage extent [Sirkar, J. et al. 1997 and Rawson et al. 1998]. The primary reason for this exclusion is that no definitive theory or data exists to define this relationship.

Figure 1 illustrates the methodology used in this study to predict the probabilistic extent of damage in collision as a function of ship structural design [Brown and Amrozowicz 1996]. Components of this methodology are described in this paper.

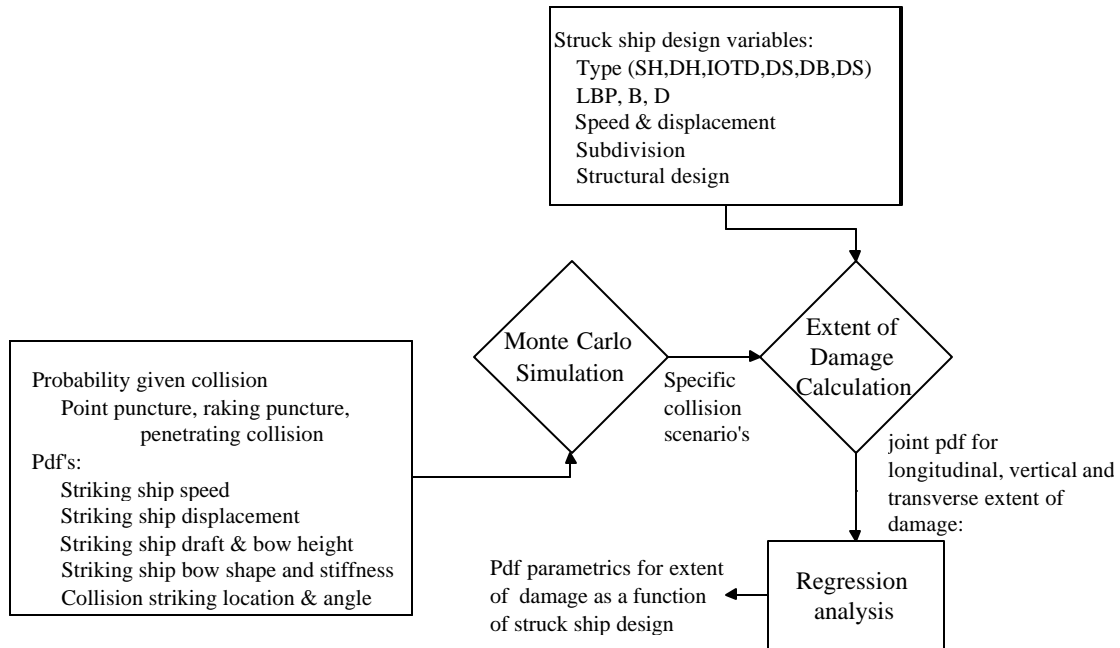


Figure 1. Method to predict probabilistic damage [Brown and Amrozowicz 1996]

The process begins with a set of probability density functions (pdfs) defining possible collision scenarios. Using these pdfs, a specific scenario is selected in a Monte Carlo simulation, and combined with a specific structural design to predict damage. This process is repeated for thousands of scenarios and a range of structural designs until sufficient data is generated to build a set of parametric equations relating probabilistic damage extent to structural design. These parametric equations can then be used in oil outflow or damage stability calculations.

2. SIMPLIFIED COLLISION MODEL (SIMCOL)

In 1979, the SSC conducted a review of collision research and design methodologies [Giannotti et al. 1979]. They concluded that the most promising simplified collision analysis alternative was to extend Minorsky's original analysis [1959] of high-energy collisions by including consideration of shell membrane energy absorption. A simple and fast model is important in probabilistic analysis because thousands of different scenarios must be run to develop statistically significant results.

A more recent review of the literature and of the applicability of available methods for predicting structural performance in collision and grounding was made at the 1997 International Ship and Offshore Structures Congress by Specialist Panel V.4

[ISSC 97]. Their report states: “Knowledge of behavior on a global level only (i.e., total energy characteristics like the pioneering Minorsky formula) is not sufficient. The designer needs detailed knowledge on the component behavior (bulkheads, girders, plating, etc.) in order to optimize the design for accident loads.”

The approach taken in this research is to progressively increase the complexity of SIMCOL starting with a modified Minorsky approach until results with sufficient accuracy and sensitivity to design characteristics are obtained. This paper presents the most recent product of this evolution.

SIMCOL uses a time-domain simultaneous solution of external ship dynamics and internal deformation mechanics similar to that originally proposed by Hutchison [1986]. Figure 2 shows the SIMCOL simulation process. The Internal Sub-Model performs Steps 2 and 3 in this process. It calculates internal deformation due to the relative motion of the two ships, and the internal reaction forces resulting from this deformation. The External Sub-Model performs Steps 1 and 4 in this process.

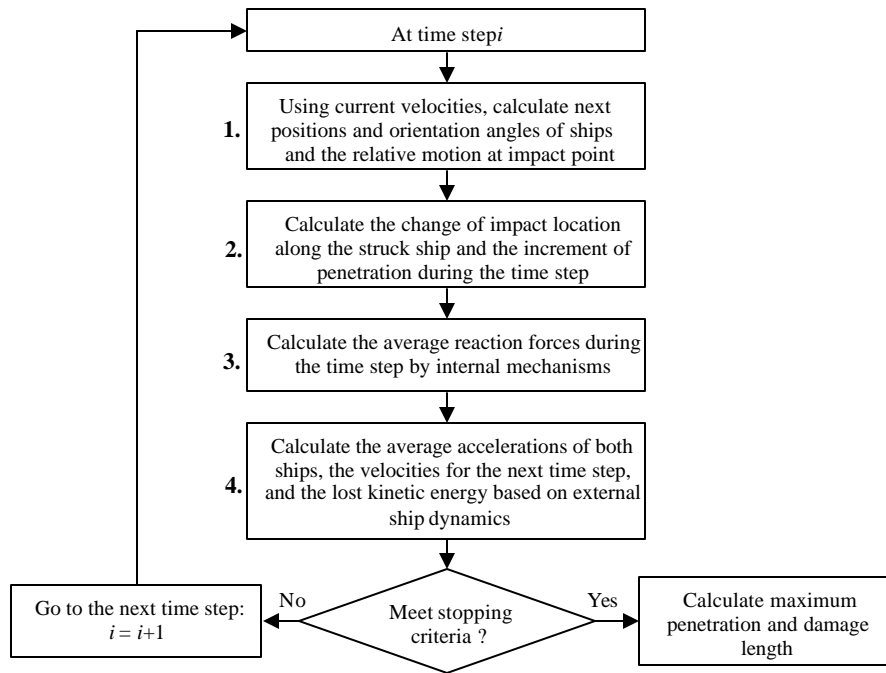


Figure 2. SIMCOL process

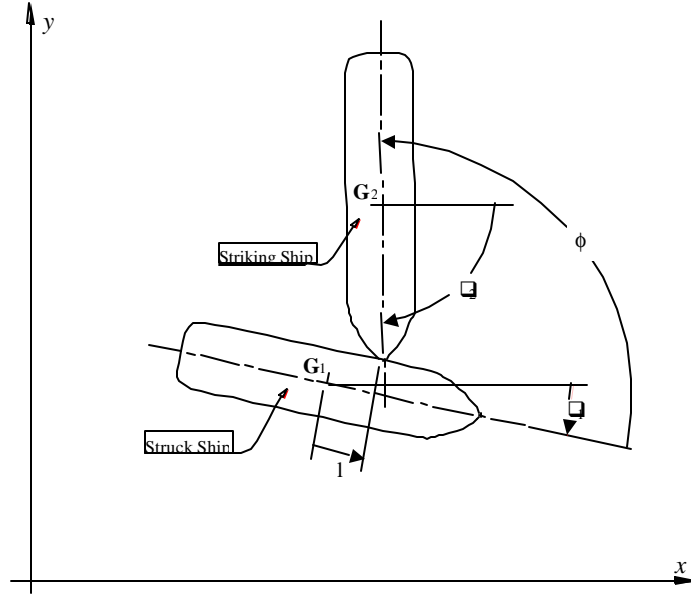


Figure 3. SIMCOL global coordinate system

The External Dynamics Sub-Model uses a global coordinate system shown in Figure 3 and local systems fixed in each ship. Its origin is at the initial ($t = 0$) center of gravity of the struck ship with the x -axis towards the bow of the struck ship. The virtual mass tensor, \mathbf{M}_{Vq} , in the global system for each ship is:

$$\mathbf{M}_{Vq} = \mathbf{M}_{ship} + \mathbf{A}_q = \begin{bmatrix} m_{V11} & m_{V12} & 0 \\ m_{V21} & m_{V22} & 0 \\ 0 & 0 & I_{V33} \end{bmatrix} \quad (1)$$

$$= \begin{bmatrix} m_s + a_{11} \cos^2 \mathbf{q} + a_{22} \sin^2 \mathbf{q} & (a_{11} - a_{22}) \cos \mathbf{q} \sin \mathbf{q} & 0 \\ (a_{11} - a_{22}) \cos \mathbf{q} \sin \mathbf{q} & m_s + a_{11} \sin^2 \mathbf{q} + a_{22} \cos^2 \mathbf{q} & 0 \\ 0 & 0 & I_{s33} + a_{33} \end{bmatrix}$$

where:

- ▶ - ship heading (degrees)
- ▶ - collision angle (degrees)
- a_{11} - added mass in the surge direction (kg)
- a_{22} - added mass in the sway direction (kg)
- a_{33} - yaw added mass moment of inertia (kg-m²)
- m_s - ship mass (kg)
- I_{s33} - ship yaw mass moment of inertia (kg-m²)

Referring to Figure 2, Step 1, the velocities from the previous time step are applied to the ships to calculate their positions at the end of the current time step:

$$\mathbf{X}_{n+1} = \mathbf{X}_n + \mathbf{V}_{sn} t \quad (2)$$

where:

- \mathbf{X} - location and orientation of ships in the global system, $\mathbf{X} = \{x, y, \blacktriangleright\}^T$

\mathbf{V}_{sn} - ship velocity, $\mathbf{V}_s = \{u, v, \dot{\psi}\}^T$

Δt - time step (seconds)

In Steps 2 and 3, the Internal Model calculates the compatible deformation, and the average forces and moments generated by this deformation over the time step. In Step 4, these forces and moments are applied to each ship. The new acceleration for each ship is:

$$\mathbf{V}'_s = \frac{\mathbf{F}}{\mathbf{M}_{VJ}} \quad (3)$$

$$u' = \frac{F_x m_{V22} - F_y m_{V12}}{m_{V11} m_{V22} - m_{V12}^2} \quad (4)$$

$$v' = \frac{F_y m_{V11} - F_x m_{V12}}{m_{V11} m_{V22} - m_{V12}^2}$$

$$w' = \frac{M}{I_{V33}}$$

where:

\mathbf{F} - forces exerted on the ships in the global system, $\mathbf{F} = \{F_x, F_y, M\}^T$

\mathbf{V}'_s - ship acceleration, $\mathbf{V}'_s = \{u', v', \dot{\psi}'\}^T$

The new velocity for each ship at the end of the time step is then:

$$\mathbf{V}_{s,n+1} = \mathbf{V}_{s,n} + \mathbf{V}'_s \Delta t \quad (5)$$

The Internal Sub-Model calculates the struck ship deformation resulting from the ships' relative motion, and calculates the average internal forces and moments generated by this deformation over the time step. Refer to Figure 2, Steps 2 and 3. The Internal Sub-Model determines reacting forces from side and bulkhead (vertical) structures using specific component deformation mechanisms including: membrane tension; shell rupture; web frame bending; shear and compression; force required to propagate the yielded zone; and friction. It determines absorbed energy and forces from the crushing and tearing of decks, bottoms and stringers (horizontal structures) using the Minorsky [1959] correlation as modified by Reardon and Sprung [1996]. Total forces are the sum of these two components. In SIMCOL Version 2.1, the striking ship bow is assumed to be rigid and wedge-shaped with upper and lower extents determined by the bow height of the striking ship and the relative drafts of the two ships. Deformation is only considered in the struck ship.

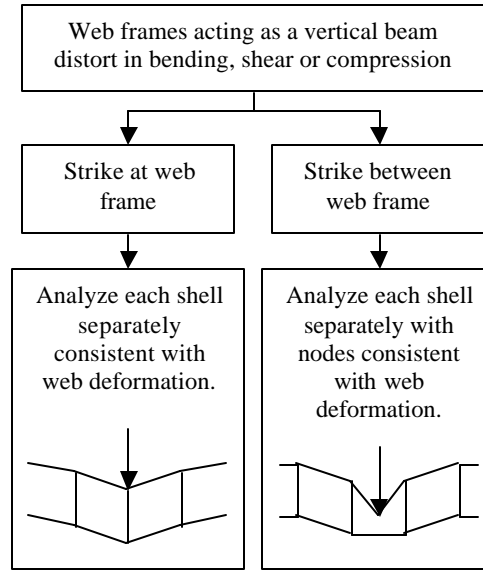


Figure 4. Web deformation cases modeled in SIMCOL [Rosenblatt 1975]

Penetration of the struck ship begins with the side shell plating and webs (vertical structures). Figure 4 illustrates the two basic types of strike determined by the strike location relative to the webs. In this analysis:

- Plastic bending of shell plating is not considered. The contribution of plastic bending in the transverse deformation of longitudinally stiffened hull plates is negligible. The sample calculation sheets in Rosenblatt [1975] support this argument. In six test cases, the energy absorbed in plastic bending never exceeds 0.55% of the total absorbed energy when the cargo boundary is ruptured. It is a good assumption that the plastic membrane tension phase starts from the beginning of collision penetration and is the primary shell energy-absorption mechanism.
- Rupture of stiffened hull plates starting in the stiffeners is not considered. This mechanism is unlikely for most structures except for flat-bar stiffened plates. It is a standard practice to use angles or bulbs instead of flat bar for longitudinal stiffeners of side shell and longitudinal bulkheads, therefore, this option is not considered in SIMCOL.
- Web frames do not yield or buckle before plates load in membrane tension. McDermott [1974] demonstrates that this mechanism is unlikely and does not contribute significantly to absorbed energy in any case. This mechanism requires very weak web frames that would not be sufficient to satisfy normal sea and operational loads.

In a right-angle collision case, equation (6) gives the total plastic energy absorbed in membrane tension in time step n . This assumes that the plate is not ruptured, that flanking webs deflect only in the transverse direction, and that compression in the side shell caused by longitudinal bending of the ship hull girder is small.

$$\begin{aligned}
 E_n &= T_m e_{tn} \\
 T_m &= s_m t B_e
 \end{aligned}
 \tag{6}$$

where:

- E_n - plastic energy absorbed by side shell or longitudinal bulkhead (J)
- T_m - membrane tension (N)
- s_m - yield stress of side shell or bulkhead adjusted for strain rate (Pa)

- e_{in} - total elongation of shell or bulkhead structure within the damaged web spacing
- t - smeared thickness of side shell or bulkhead plating and stiffeners (m)
- B_e - effective breadth (height) of side shell or bulkhead (m)

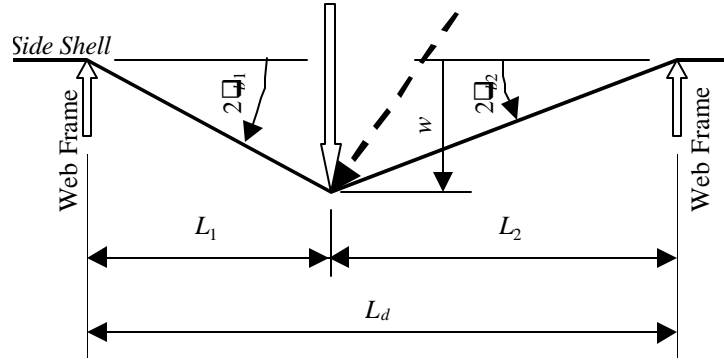


Figure 5. Membrane geometry

Figure 5 illustrates the membrane geometry for calculation of elongation where e_1 and e_2 are the elongation of legs L_1 and L_2 respectively:

$$e_i = \sqrt{L_i^2 + w^2} - L_i \cong \frac{w^2}{2L_i} \quad (7)$$

$$e_t = e_1 + e_2 = \frac{L_d}{2L_1L_2} w^2$$

and:

- L_d - distance between adjacent webs (m)
- w_n - transverse deflection at time step n (m)

Side shell rupture due to membrane tension is predicted using the following criteria:

- The strain in the side shell reaches the rupture strain, ϵ_r , which is taken as 10% in ABS steel; or
- The bending angle at a support reaches the critical value as defined in equation (8) [Rosenblatt 1975].

$$e_m = \frac{4}{3} \frac{s_m}{s_u - s_m \cos q_c} \sin q_c \tan q_c = 1.5D \quad (8)$$

where:

- ▶ m - maximum bending and membrane-tension strain to rupture
- ▶ m - membrane-tension in-plate stress (MPa)
- ▶ u - ultimate stress of the plate (MPa)
- ▶ c - critical bending angle
- D - tension test ductility

The resistance of the membrane is only considered up to the point of rupture:

$$e_i = \frac{e_i}{L_i} \leq e_r \quad (9)$$

$$q_{bi} = \frac{1}{2} \arctan \frac{w}{L_i} \cong \frac{w}{2L_i} \leq q_c$$

where:

- ▶ ϵ_i - strain in leg i
- ▶ β_{bi} - bending angle of flanking web frames

Since the striking bow normally has a generous radius, the bending angle at the impact location is not considered in the rupture criteria. From these equations, it is seen that only the strain and bending angle in the shorter leg need be considered for right angle collisions. Based on material properties of ABS steel, the critical bending angle β_c from equation (8) is 19.896, 17.318 or 16.812 degrees for MS, H32 or H36 grades respectively. Once either of the rupture criteria is reached, the side shell or longitudinal bulkhead is considered ruptured, and does not continue to contribute to the reacting force.

For collisions at an oblique angle, the membrane tension is only fully developed in the leg behind the strike, L_2 in Figure 5. This is demonstrated in the force diagram shown in Figure 6, where T_1 is much smaller than T_2 . It is also assumed that all the strain developed from membrane tension is behind the striking point. Therefore, the first rupture criterion in equation (9) becomes:

$$\epsilon_b = \frac{\epsilon_t}{L_b} \leq \epsilon_r \quad (10)$$

where ϵ_b and L_b represent the strain and length of the leg behind the strike.

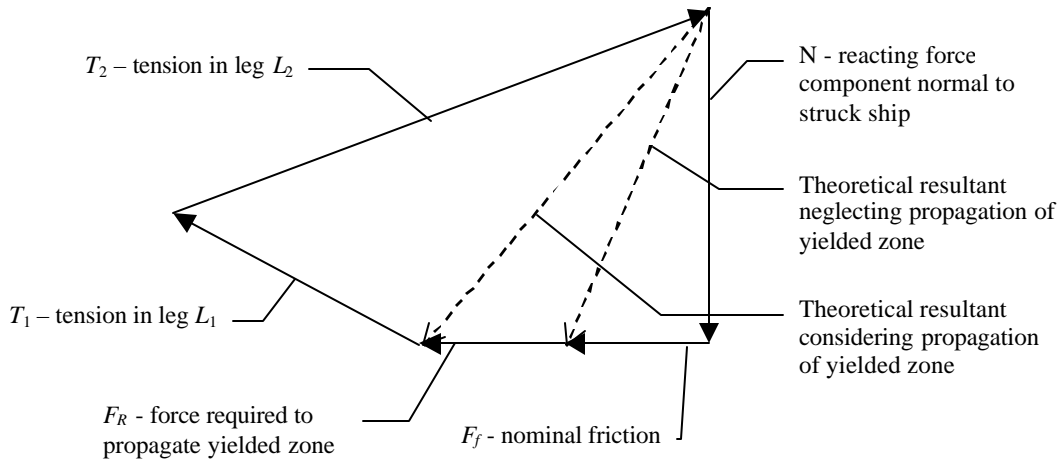


Figure 6. Oblique collision force diagram [McDermott 1974]

Web failure modes include bending, shear, and compression. Web frames are allowed transverse deformation while keeping their longitudinal locations. The resisting force is assumed constant at a distorted flanking web frame, and the transverse deformation of the web frame is assumed uniform from top to bottom. The magnitude of this force is its maximum elastic capacity. From Figure 6, the applied force on a rigid flanking web frame is:

$$P_i = T_i \frac{w}{L_i} \quad (11)$$

where P_i and T_i are referred to the particular leg L_i . If the applied force, P_i , is greater than the maximum elastic capacity of the flanking web, P_{wf} , the particular web frame is deformed as shown in Figure 7. The change of angle, α_c , at the distorted web is then:

$$\mathbf{g}_{ci} \equiv \frac{P_{wf}}{T_i} \quad (12)$$

Rosenblatt [1975] proposed an approach to determine whether P_i exceeds the capacity P_{wf} , and to estimate the value of P_{wf} . First, the allowable bending moment and shear force of the web frame at each support, the crushing load of the web, and the buckling force of supporting struts are calculated. Then, the load P_i is applied to the web frame, and the induced moments, shear forces and compression of the web frame and struts are calculated, considering the web frame as a beam with clamped ends. The ratios of the induced loads to the allowable loads are determined using equation (13). If the maximum ratio, R_m , is greater than unity, the load, P , exceeds the capacity, and the web frame deforms. R_m is also used to estimate the number of distorted web frames.

$$R_m = \frac{P}{P_{wf}} \quad (13)$$

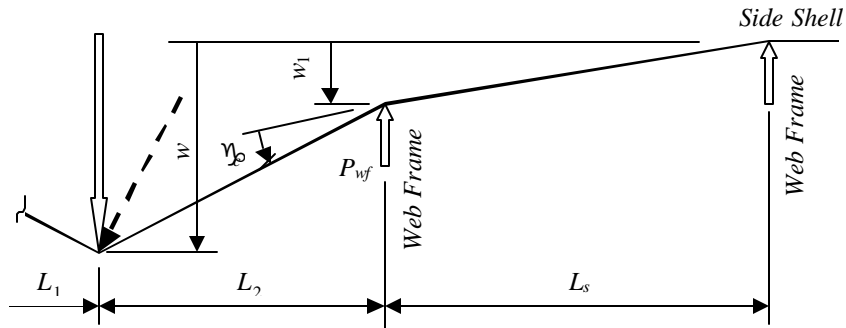


Figure 7. Deflection and forces in web frames

The deflection at the outermost distorted web is:

$$w_n = \frac{L_s}{L_i + nL_s} \left\{ w - \mathbf{g}_{c2} \left[nL_i + \frac{1}{2}(n-1)nL_s \right] \right\} \quad (14)$$

where:

n - number of deformed web frames on L_i side

L_s - web frame spacing (m)

The deflection at other deformed web frames is:

$$w_j = (n-j+1)w_n + \frac{1}{2}(n-j)(n-j+1)\mathbf{g}_{c2}L_s \quad (15)$$

where j is the number of webs counted from the striking point. The elongation in adjacent webs is:

$$e_j = \sqrt{(w_j - w_{j+1})^2 + L_s^2} - L_s \quad (16)$$

and the elongation in the struck web is:

$$e_{0i} = \sqrt{(w - w_1)^2 + L_i^2} - L_i \quad (17)$$

With these elongation and deformation results, the rupture criteria given in equations (9) and (10) are applied to all deformed webs. The total elongation on the L_i side is:

$$e_{ti} = e_{0i} + \sum_{j=1}^n e_{ji} \quad (18)$$

and the energy absorbed in membrane tension and web deformation is:

$$E_i = T_i e_{ti} + P_{wf} \sum_{j=1}^n w_{ji} \quad (19)$$

For right angle collisions, T_i always equals T_m as calculated in equation (6). In oblique angle collisions, T_i equals T_m if L_i is on the side behind the strike. Based on experimental data, Rosenblatt [1975] suggests using $\frac{1}{2} T_m$ ahead of the strike and this is used in SIMCOL.

For double hull ships, if the web frames are distorted because of bending, shearing and buckling of supporting struts, the deformed web frames push the inner skin into membrane tension as shown in Figure 4 (right), and the right angle collision mechanism is applied to the inner hull. Inner skin integrity is checked using equations (9) and (10), and the energy absorbed in inner-skin membrane tension is calculated using equation (6).

In the simulation, the energy absorbed in membrane tension and web deformation during the time step is:

$$\Delta KE_n = (E_{1,n+1} + E_{2,n+1}) - (E_{1n} + E_{2,n}) \quad (20)$$

Considering the friction force, F_f , shown in Figure 6, and assuming the dynamic coefficient of friction is a constant value of 0.15, the reacting forces and moments are:

$$\begin{aligned} \Delta KE_n &= N_n (w_{n+1} - w_n) + F_{fn} |l_{n+1} - l_n| = N [(w_{n+1} - w_n) + 0.15 |l_{n+1} - l_n|] \\ F_{hn} &= N_n = \frac{(E_{1,n+1} + E_{2,n+1}) - (E_{1n} + E_{2,n})}{(w_{n+1} - w_n) + 0.15 |l_{n+1} - l_n|} \\ F_{xn} &= F_f \frac{(l_{n+1} - l_n)}{|l_{n+1} - l_n|} = 0.15 F_{hn} \frac{(l_{n+1} - l_n)}{|l_{n+1} - l_n|} \\ M_n &= -F_{xn} d_n + F_{hn} l_n \end{aligned} \quad (21)$$

In addition to the friction force, another longitudinal force, F_R , the force to propagate the yielding zone, is considered, as shown in Figure 6. McDermott [1974] provides an expression for this force:

$$F_R = \frac{s_y d'}{R} \left[d t_w \left(1 - \frac{s_y R}{d' E} \right)^2 + t_f (b - t_w) \left(\frac{d' - 0.5 t_f}{d'} - \frac{s_y R}{d' E} \right) \right] \quad (22)$$

where:

- d - depth of side shell longitudinal stiffeners
- R - radius of the striking bow
- t_w - thickness of side shell stiffener webs
- t_f - thickness of side shell stiffener flanges
- b - width of side shell stiffener flanges
- E - modulus of elasticity

or when simplified:

$$\begin{aligned} c_F &= \frac{F_R}{s_y A_{stiff}} \\ c_A &= \frac{A_{stiff}}{A_{total}} \\ F_R &= c_F c_A s_y t B \end{aligned} \quad (23)$$

where:

- c_F - force coefficient;
- c_A - ratio of sectional areas;
- A_{stiff} - sectional area of stiffeners; and
- A_{total} - total sectional area of stiffeners and their attached plate.

The full implementation of equations (22) and (23) requires structural details that are not appropriate for this simplified analysis. In this study, based on a sampling of typical side shell scantlings, a simplified calculation is used where $c_F \rightarrow c_A$ is assumed to have a constant value of 0.025.

Since F_R also effects membrane tension energy, equation (21) becomes:

$$\begin{aligned} \Delta KE_n &= F_{lm} [(w_{n+1} - w_n) + 0.15 |l_{n+1} - l_n|] + F_R (l_{n+1} - l_n) \\ F_{lm} &= \frac{(E_{1,n+1} + E_{2,n+1}) - (E_{1n} + E_{2,n}) - F_R (l_{n+1} - l_n)}{(w_{n+1} - w_n) + 0.15 |l_{n+1} - l_n|} \\ F_{xn} &= (F_R + 0.15 F_{lm}) \frac{(l_{n+1} - l_n)}{|l_{n+1} - l_n|} \\ M_n &= -F_{xn} d_n + F_{lm} l_n \end{aligned} \quad (24)$$

The Internal Sub-Model determines absorbed energy and forces from the crushing and tearing of decks, bottoms and stringers (horizontal structures) in a simplified manner using the Minorsky [1959] correlation as modified by Reardon and Sprung [1996].

V.U. Minorsky conducted the first and best known of the empirical collision studies based on actual data. His method relates the energy dissipated in a collision event to the volume of damaged structure. Actual collisions in which ship speeds,

collision angle, and extents of damage are known were used to empirically determine a linear constant. This constant relates damage volume to energy dissipation. In the original analysis the collision is assumed to be totally inelastic, and motion is limited to a single degree of freedom. Under these assumptions, a closed form solution for damaged volume can be obtained. With additional degrees of freedom, a time-stepped solution must be used.

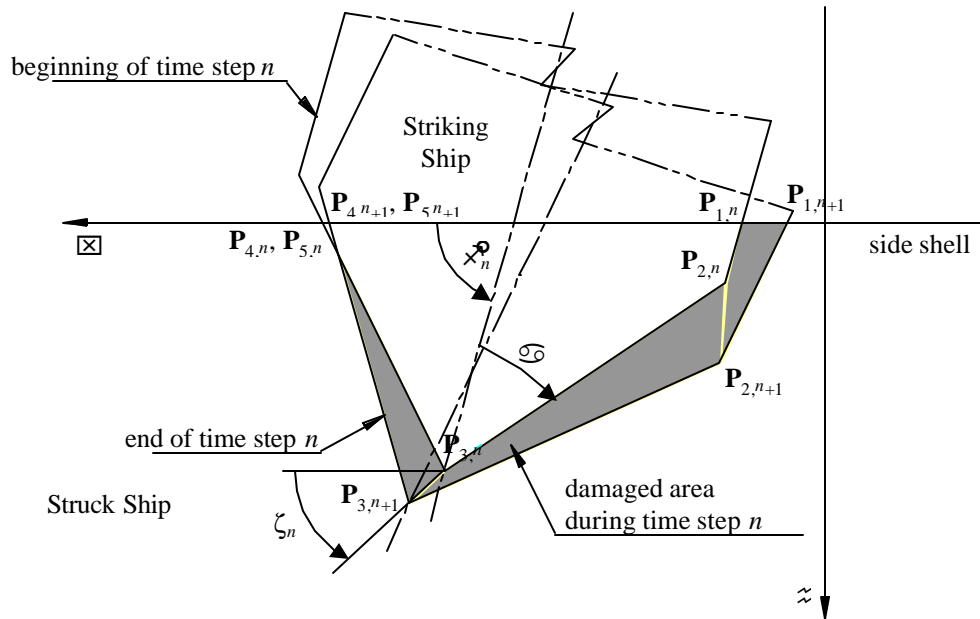


Figure 8. Sweeping segment method

Step 2 in the collision simulation process calculates damaged area and volume in the struck ship given the relative motion of the two ships in a time step calculated in Step 1 by the External Sub-Model. Figure 8 illustrates the geometry of the sweeping segment method used for this calculation in SIMCOL.

The intrusion portion of the bow is described with five nodes, as shown in Figure 8. The shaded area in Figure 8 shows the damaged area of decks and/or bottoms during the time step. Coordinates of the five nodes in the $x-z$ system at each time step are derived from the penetration and location of the impact, the collision angle, α , and the half entrance angle, ζ , of the striking bow.

The damaged plating thickness t is the sum thickness of deck and/or bottom structures that are within the upper and lower extents of the striking bow. Given the damaged material volume, the Minorsky force is calculated based on the following assumptions:

- The resistant force acting on each out-sweeping segment is in the opposite direction of the average movement of the segment. The force exerted on the struck ship is in the direction of this average movement.
- The work of the resistant force is done over the distance of this average movement.
- The total force on each segment acts through the geometric center of the sweeping area.

The energy absorbed is then:

$$\Delta KE_{1,n} = 47.1 \times 10^6 R_{T1,n} = 47.1 \times 10^6 A_{1,n} t \quad (25)$$

where:

- ▀ ΔKE - kinetic energy absorbed by decks, bottoms and stringers (J)
- R_T - damaged volume of structural members (m³)
- A - damaged area of the decks or bottoms swept by each bow segment (m²)
- t - total thickness of impacted decks or bottoms (m)

Forces and moments acting on other segments are calculated similarly. The total exerted force, \mathbf{F}_n , is the sum of the forces and moments on each segment:

$$\mathbf{F}_n = \sum_{i=1}^4 \{F_{xi,n}, F_{hi,n}, M_{i,n}\} \quad (26)$$

These forces are added to the side shell, bulkhead and web forces. Internal forces and moments are calculated for the struck ship in the local coordinate system and transformed to the global system. The forces and moments on the striking ship have the same magnitude and the opposite direction of those acting on the struck ship.

3. COLLISION SCENARIOS

A collision scenario is described using random variables with varying degrees of dependency. The data sources used to determine the probabilities and probability density functions necessary to define these random variables were obtained from a number of sources [Sandia National Laboratories 1998; Lloyds 1993; ORI 1980; ORI 1981 and Engineering Computer Optecnomics, Inc (ECO) 1996]. In this paper pdfs generated from this data are used to develop 10000 collision cases that are applied to four struck tanker designs, for a total of 40000 SIMCOL runs. SIMCOL calculates damage penetration, damage length, oil outflow and absorbed energy for each of these runs.

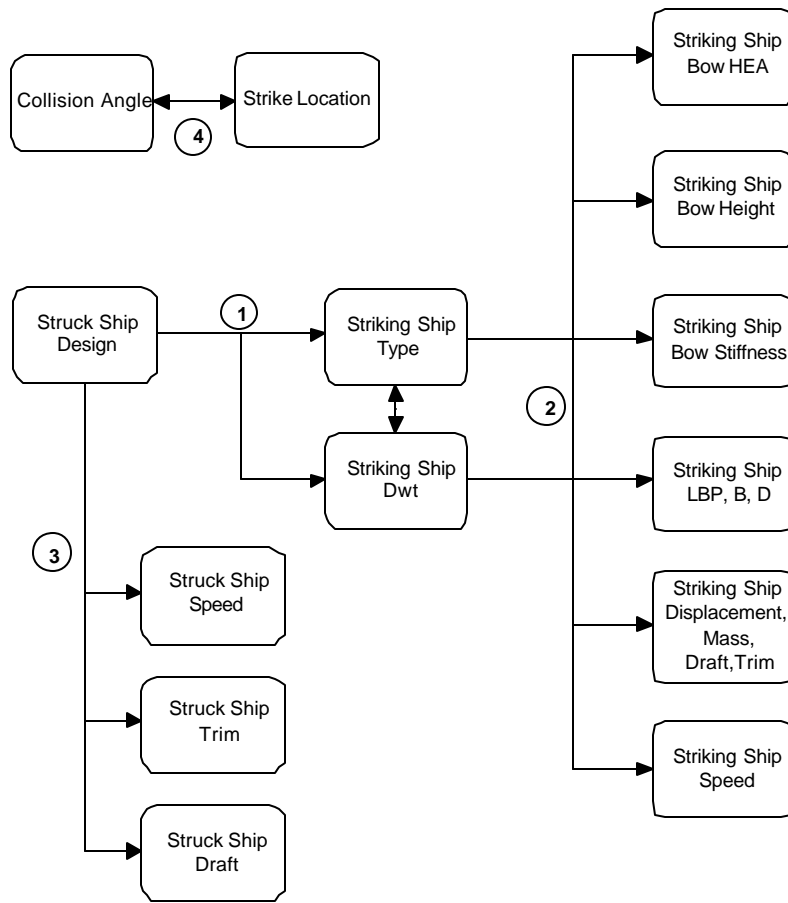


Figure 9. Collision event variables

Collision event variables are not expected to be independent, but their interdependence is difficult to quantify because of limited collision data. Figure 9 provides a framework for defining the relationship of scenario variables. Available data is incomplete for quantifying this relationship. Strike location must often be inferred from the damage description because reliable records of the precise location are not available. Ship headings and speeds prior to the collision are often included in accident reports, but collision angle and ship speed at the moment of collision are frequently not included or only estimated and described imprecisely.

Figure 10 provides probabilities of the struck ship encountering specific ship types. These probabilities are based on the fraction of each ship type in the worldwide ship population in 1993 [Lloyds 1993]. Each of the general types includes a number of more specific types:

- Tankers – includes crude and product tankers, ore/oil carriers, LPG tankers, chemical tankers, LNG tankers, and oil/bulk/ore carriers
- Bulk carriers - includes dry bulkers, ore carriers, fish carriers, coal carriers, bulk/timber carriers, cement carriers and wood chip carriers
- Cargo vessels (Break Bulk / Freighters) – includes general freighters and refrigerated freighters
- Passenger – includes passenger and combo passenger/cargo ships

- Containerships – includes containerships, car carriers, container/RO-ROs, ROROs, bulk/car carriers, and bulk/containerships

It is likely that particular ships are more likely to meet ships of the same type since they travel the same routes, but this relationship could not be established with available data. Additional collision data must be obtained to establish this relationship.

Figure 11 shows the worldwide distributions of displacement for these ship types.

Collision speed is the striking ship speed at the moment of collision. It is not necessarily related to service speed. It depends primarily on actions taken just prior to collision. Collision speed data is collected from actual collision events. Figure 12 is a plot of data derived from the Sandia Report [1998] and limited USCG tanker-collision data [USCG 1990].

Regression curves were developed from Lloyds data [1993] for length, beam, draft, and bow height as a function of striking ship type and displacement. Typical principal characteristic data is shown in Figure 13. Bow half-entrance angle is not a standard ship principal characteristic. A limited number of bow drawings were reviewed in the Sandia Study [1998] and half-entrance values were derived for each type of ship. These values are used in SIMCOL.

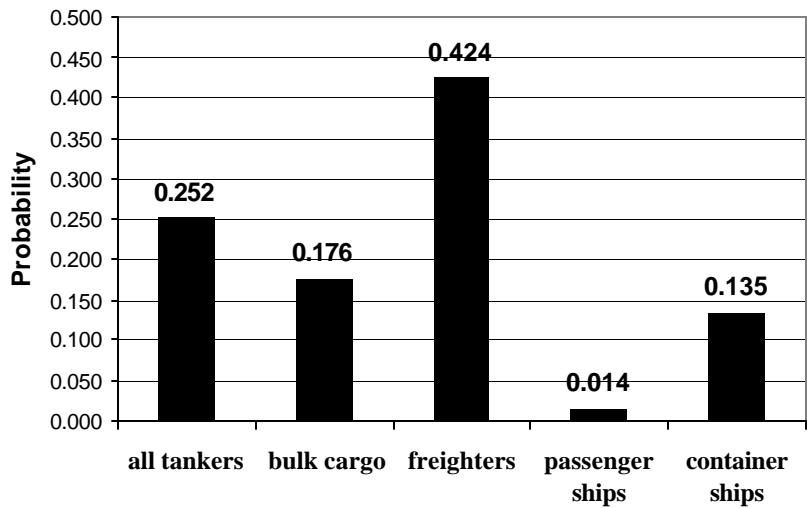


Figure 10. Striking ship type probability

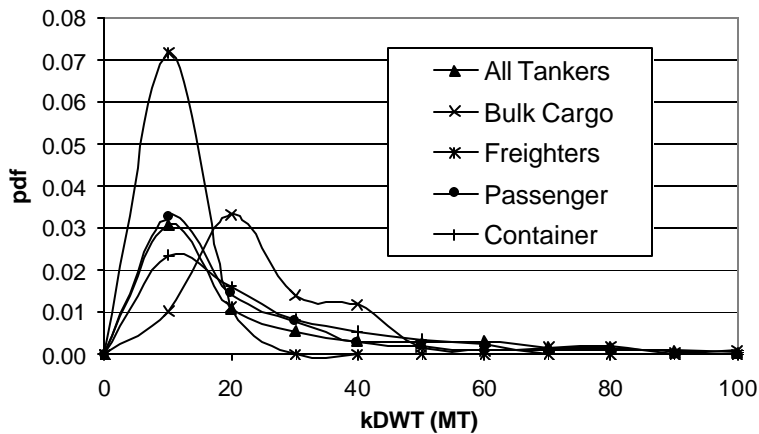


Figure 11. Striking ship displacement, worldwide

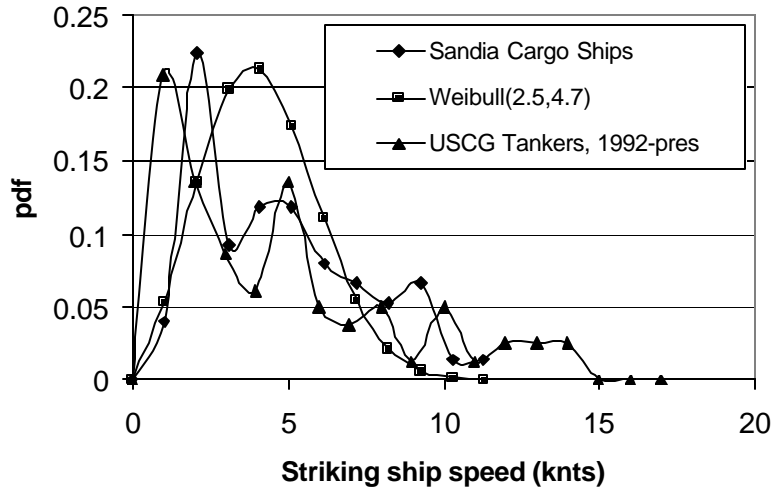


Figure 12. Striking Ship Speed (knots)

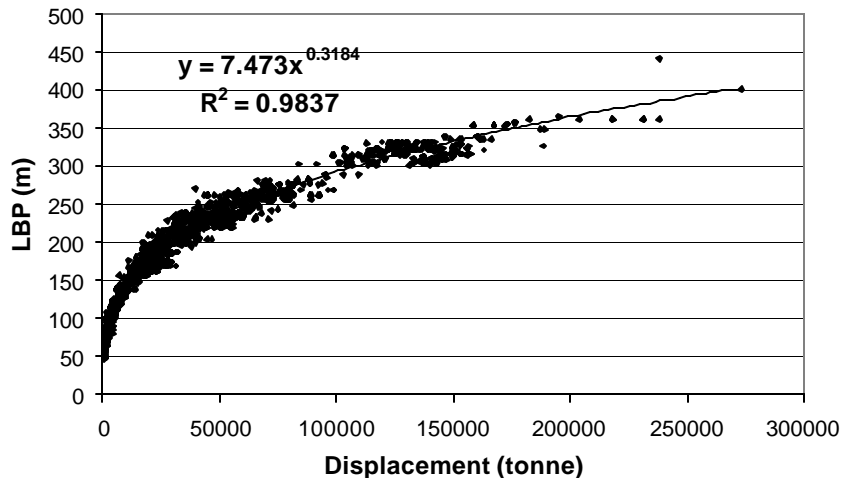


Figure 13. Worldwide tankers: length vs. displacement

Figure 14 is a plot of struck ship speed derived from the USCG tanker collision data [USCG 1990]. The struck ship collision speed distribution is very different from service speed. Struck ships are frequently moored or at anchor as is indicated by the significant pdf value at zero speed.

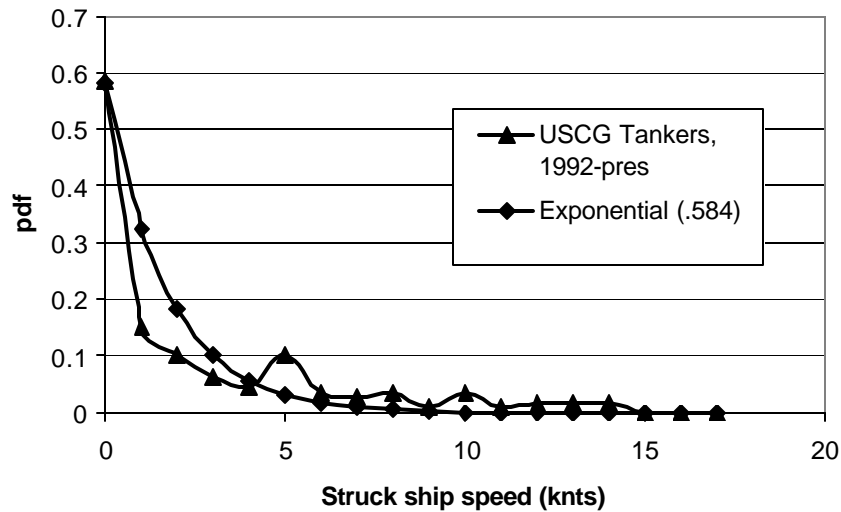


Figure 14. Struck ship speed (knts)

An approximate Normal distribution ($\mu = 90$ degrees, $\sigma = 28.97$ degrees) is fit to collision angle data derived from the Sandia Report [1998], and is used to select collision angle in the Monte Carlo simulation. At more oblique angles, there is a higher probability of ships passing each other or only striking a glancing blow. These cases are frequently not reported.

The current IMO pdf for strike longitudinal location specifies a constant value over the entire length of the struck ship, IMO [1995]. The constant pdf was chosen for convenience and because of the limited available data. Figure 15 shows a bar chart of the actual data used to develop the IMO pdf, IMO [1989], and data gathered for cargo ships in the Sandia Study. This data does not indicate a constant pdf. The IMO data is from 56 of 200 significant tanker-collision events for which the strike location is known. The Sandia data indicates a somewhat higher probability of midship and forward strikes compared to the IMO data. The IMO tanker probabilities are used in SIMCOL.

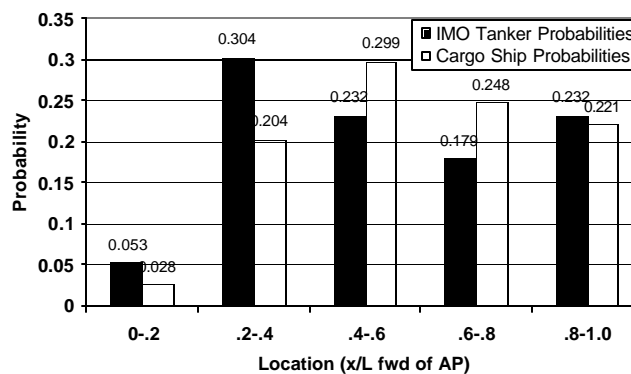


Figure 15. Longitudinal damage location probabilities

4. RESULTS AND DISCUSSION

Four struck ships are used in the preliminary application of this method. The ships include two 150k dwt oil tankers, one single hull and one double hull, and two 45k dwt oil tankers, one single hull and one double hull. SIMCOL input data for these ships are provided in Table 1 and Table 2. Collision scenario pdfs are used to develop 10000 collision cases that are

applied to each of the four ships. SIMCOL calculates damage penetration, damage length and absorbed energy for each of these cases.

Table 1. Struck ship principal characteristics

	DH150	SH150	DH45	SH45
Displacement, MT	151861	152395	47448	47547
Length, m	261.0	266.3	190.5	201.2
Breadth, m	50.0	50	29.26	27.4
Depth, m	25.1	25.1	15.24	14.3
Draft, m	16.76	16.76	10.58	10.6
Double bottom height, m	3.34	NA	2.1	NA
Double hull width, m	3.34	NA	2.438	NA

Table 2. Struck ship structural characteristics

	DH150	SH150	DH45	SH45
Web frame spacing ,mm	5.2	5.2	3.505	3.89
Smeared deck thickness, mm	29.4	28.2	27.6	30.5
Smeared inner bottom thickness, mm	37.1	NA	27.8	NA
Smeared bottom thickness, mm	36.6	44.2	34	38.5
Smeared stringer thickness, mm	14.9	NA	NA	NA
Smeared side shell thickness, mm	26.7	27.8	24.5	23.6
Smeared inner side thickness, mm	28.1	NA	20.1	NA
Smeared long bhd thickness, mm	25.1	24.5	20	33.4
Smeared upper web thickness	12.5	12.5	12.7	19
Smeared lower web thickness	14.5	16	12.7	19

Figure 16 and Figure 17 are the resulting probability density functions for damage penetration and damage length. Table 3 lists mean values for scenario variables, damage penetration, and damage length. The damage pdfs for the four struck ships are quite similar. Unlike the IMO standard pdfs, penetration in these pdfs is not normalized with breadth. The larger struck ships must absorb more energy due to their higher inertia, but structural scantlings are also larger so damage penetrations and lengths for the 150k dwt ships are similar to the 45k dwt ships. Comparing the mean values in Table 3, on the average, the single hull ships do have larger penetrations and damage lengths than the double hull ships, and the larger ships have larger penetrations and damage lengths than the smaller ships.

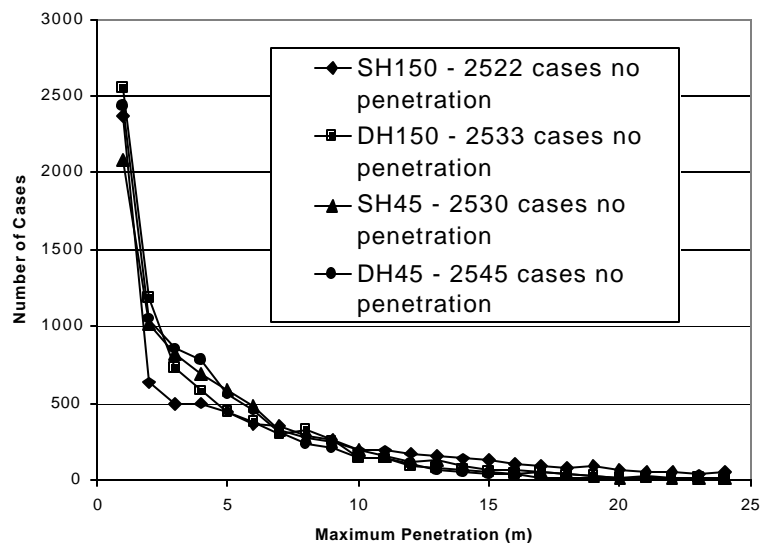


Figure 16. Damage penetration pdf

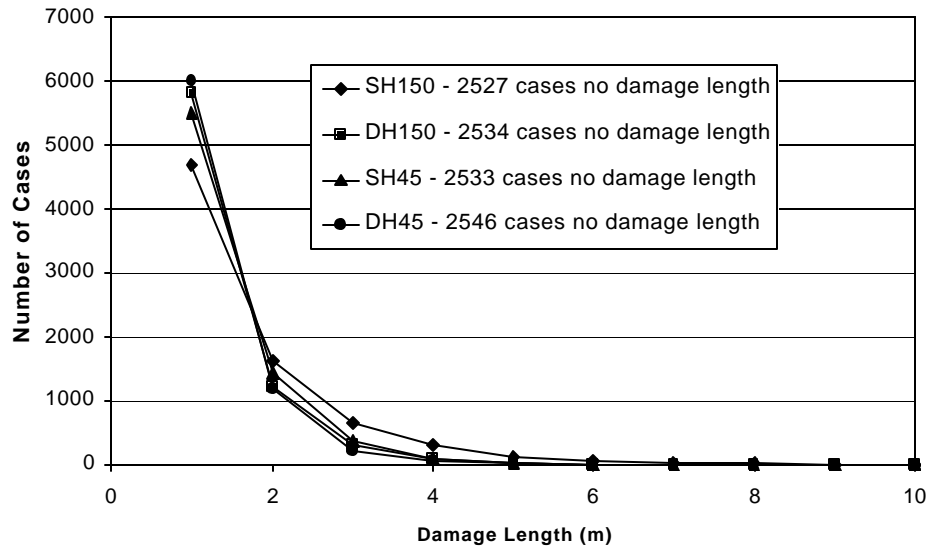


Figure 17. Damage length pdf

Table 3. Mean scenario and damage values

	All	DH150	SH150	DH45	SH45
Mean Struck Ship Velocity (knots)	2.49				
Mean Striking Ship Velocity (knots)	4.27				
Mean Strike Location (x/L)	0.47				
Mean Collision Angle	90.00				
Mean Striking Ship Displacement (tonne)	13660.00				
Mean Damage Penetration (meters)		1.385	2.28	1.281	1.571
Mean Damage Length (meters)		2.523	3.87	2.291	2.809

5. CONCLUSIONS AND FUTURE WORK

This paper presents a rational method for predicting struck-ship damage extent pdfs in ship collisions. Such a method is essential to consider crashworthiness in future oil outflow and damage stability regulations. The next step in this research is to apply SIMCOL to a wide range of tanker structural designs and attempt to develop a direct parametric relationship between structural design and probabilistic damage extents. This is the last step of the method presented in Figure 1. Further development and validation of SIMCOL is ongoing.

REFERENCES

- Brown, A.J., Tikka, K., Daidola, J.C., Lutzen, M., Choe, I.H. 2000, Structural Design and Response in Collision and Grounding, *SNAME Transactions* **108**, 447-473.
- Brown, A. and Amrozowicz, M. 1996, Tanker Environmental Risk - Putting the Pieces Together, *SNAME/SNAJ International Conference on Designs and Methodologies for Collision and Grounding Protection of Ships*.
- Chen, D. 2000, Simplified Collision Model (SIMCOL), Dept. of Ocean Engineering, Virginia Tech, Master of Science Thesis.
- Engineering Computer Optecnomics, Inc (ECO) 1996, World Fleet Data.

- Giannotti, J.G., Johns, N., Genalis, P. and Van Mater, P.R. 1979, Critical Evaluations of Low-Energy ship Collision Vol. I - Damage theories and Design Methodologies, *Ship Structure Committee Report No. SSC-284*.
- Gilbert, R. and Card, J.C. 1990, The New International Standard for Subdivision and Damage Stability of Dry Cargo Ships, *Marine Technology* **27** (2), 117-127.
- Hutchison, B.L. 1986. Barge Collisions, Rammings and Groundings - an Engineering Assessment of the Potential for Damage to Radioactive Material Transport Casks, *Report No. SAND85-7165 TTC-05212*.
- IMCO 1973, *Regulations on Subdivision and Stability of Passenger Ships as Equivalent to Part B of Chapter II of the International Convention for the Safety Of Life At Sea*, IMCO Resolution A.265 (VIII), adopted November 20, 1973.
- IMO 1989, Distribution of Actual Penetrations and Damage Locations Along Ship's Length for Collisions and Groundings, *IMO Comparative Study on Oil Tanker Design*, IMO Paper MEPC 32/7/15, Annex 5.
- IMO 1995, Interim Guidelines for Approval of Alternative Methods of Design and Construction of Oil Tankers under Regulation 13F(5) of Annex I of MARPOL 73/78, *Resolution MEPC 66 (37)*, adopted September 14, 1995.
- ISSC 1997, Report by Specialist Panel V.4 – Structural Design Against Collision and Grounding, *Proceedings of the 13th International Ship and Offshore Structures Congress 1997*, Trondheim, Norway.
- Lloyds 1993, Worldwide Ship Data, provided by MARAD.
- McDermott, J.F., Kline, R.G., Jones, E.L., Maniar, N.M., Chiang, W.P. 1974, Tanker Structural Analysis for Minor Collisions, *SNAME Transactions* **82**, 382-414.
- Minorsky, V. V. 1959, "An Analysis of Ship Collisions with Reference to Protection of Nuclear Power Plants", *Journal of Ship Research*.
- ORI 1980. Hazardous Environment Experienced by Radioactive Material Packages Transported by Water, Silver Spring, MD.
- ORI 1981. Accident Severity's Experienced by Radioactive Material Packages Transported by Water, Silver Spring, MD.
- Rawson, C., Crake, K. and Brown, A.J. 1998, Assessing the Environmental Performance of Tankers in Accidental Grounding and Collision, *SNAME Transactions* **106**, 41-58.
- Reardon, P. and Sprung, J.L. 1996, Validation of Minorsky's Ship Collision Model and Use of the Model to Estimate the Probability of Damaging a Radioactive Material Transportation Cask During a Ship Collision, *Proceedings of the International Conference on Design and Methodologies for Collision and Grounding Protection of Ships*, San Francisco.
- Rosenblatt & Son, Inc. 1975, Tanker Structural Analysis for Minor Collision, USCG Report, CG-D-72-76.
- Sandia National Laboratories 1998, Data and Methods for the Assessment of the Risks Associated with the Maritime Transport of Radioactive Materials Results of the SeaRAM Program Studies, SAND98-1171/2, Albuquerque, NM.
- Sirkar, J., Ameer, P., Brown, A.J., Goss, P., Michel, K., Willis, W. 1997, A Framework for Assessing the Environmental Performance of Tankers in Accidental Grounding and Collision, *SNAME Transactions* **105**, 253-295.
- USCG 1990, Ship Casualty Data 1982-1990.